Sharma, R. K., and R. D. Srivastava, "V_2O_5-K_2SO_4-Silica System: II. Correlation with Toluene Oxidation Activity," *J. Catalysis*.

Sharma, R. K., "Structure and Catalytic Activity of Silica Supported V_2O_5-Alkalimetal Sulphates," Ph.D. Thesis, Indian Inst. of Tech., Kanpur (1980).

Simard, G. L., J. F. Segel, R. J. Arnot, and L. A. Siegel, "Vanadium Oxides as Oxidation Catalysts," *Ind. Eng. Chem.*, **47**, 1424 (1955).

Tandy, G. H., "The Role of Alkalimetal Sulphates in Vanadium Catalysts for SO_2 Oxidation," *J. Appl. Chem.*, **6**, 68 (1956).

Yang, K. H., and O. A. Hougen, "Determination of Mechanism of Catalyzed Gaseous Reactions," *Chem. Eng. Progr.*, **46**, 146 (1950).

Manuscript received February 19, 1980; revision received May 5, and accepted May 12, 1980.

Distribution Equilibrium Between a Bulk Phase and Small Pores

The pore-bulk distribution coefficient *K* for a solute species is calculated by modelling the solute molecules as hard spheres. *K* is expanded in a virial-type series in powers of the bulk-phase concentration. The leading term is the Henry's law constant. The next two coefficients are reported for three pore shapes.

E. D. GLANDT

Department of Chemical Engineering
University of Pennsylvania
Philadelphia, Pennsylvania 19104

SCOPE

The phase equilibrium between pore and bulk solutions is relevant to several separation processes, such as adsorption, exclusion (gel-permeation) chromatography, and membrane transport. Of particular interest is the case of micropores, i.e. of pores whose characteristic linear dimension is within one order of magnitude of the size of the solute molecules. In many cases, the equilibrium between pore and bulk phases is dominated by an adsorptive (attractive) or a repulsive field exerted by the walls of the pore. Even in the absence of any such field, a partition process occurs due to the finite size of the solute molecules, which creates an exclusive region adjacent to the pore walls. All of these effects result from the interaction of single, isolated molecules with the pore walls, and are well understood. They correspond to the Henry's law regime, of proportionality between the concentrations in the bulk and in the pore. The present paper deals with the solute-solute interactions within the pore, which are important at all but the lowest concentrations, although they have been ignored to date. Because of these interactions, the distribution coefficient becomes concentration-dependent. Our goal has been to elucidate the nature of this dependence for micropores of three different shapes: a flat slit, an infinitely long circular cylinder and a spherical cavity.

CONCLUSIONS AND SIGNIFICANCE

The pore-bulk distribution coefficient for a single solute whose molecules are modeled as hard elastic spheres can be expressed as a series in powers of the bulk concentration, Eq. 29 in this work. The leading term of this expansion is the Henry's law constant, and corresponds to the well-known steric exclusion effect due to the finite size of the molecules. The next two coefficients in the series were calculated. The calculation was done analytically for the case when the pore is shaped as a flat slit, and numerically for cylindrical and spherical pores. These coefficients are the most important results of the present research, and are shown as Eq. 34 and 35 and in Tables 2 and 3.

Often the distribution coefficients determined experimentally are found to be larger than the simple steric-exclusion value, and the difference is generally explained in terms of attractive forces (adsorption) due to the pore walls, or to changes in molecular configurations. The results reported here, which apply to pores with hard, nonadsorbing walls, introduce the effect of solute-solute interactions within the pores. They can be used to discriminate whether adsorption indeed exists, and to decide on its importance.

INTRODUCTION

This work deals with the properties of pure fluids and of molecular and colloidal solutions contained inside micropores, i.e. pores whose characteristic linear dimensions are comparable to the size of the fluid molecules (in the case of pure fluids) or to the size of the solute molecules or particles (in the case of solutions). The partition or distribution equilibrium between the pore and bulk phases is extremely relevant to various adsorption processes, to exclusion (gel permeation) chromatography, and to membrane transport and separations. The problems of the distribution of a pure fluid and of a single solute in solution can be described by formally identical equations, as we shall see below. The results presented here, however, are based on the properties of hard spheres and are thus of much greater relevance to the case of nonelectrolytic solutes. Consequently, we shall favor the language of solutions and refer to the distribution of solute molecules or particles.

The distribution coefficient is defined as the ratio of the average concentration inside the pore to the concentration of the bulk phase in equilibrium with it. The average intrapore concentration, however, is not a uniquely defined quantity, since it

---

0001-1541-81-4217-0051-\$2.00.

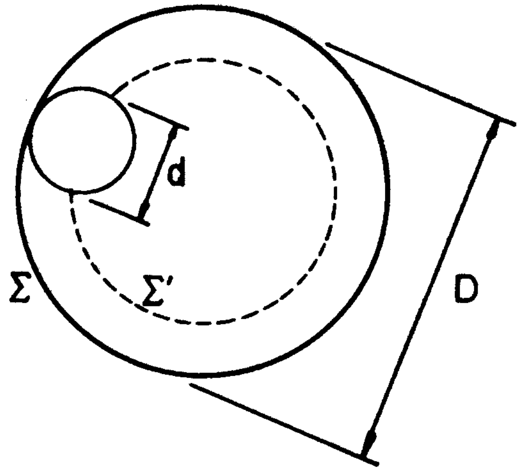

Figure 1. A schematic section of hard-spherical solute particles in a pore.

is the ratio of the (unambiguous) total number of solute moles or molecules contained within the pore to the volume of the pore. The latter quantity must be always specified, since it can be defined in several ways, and the differences between the various definitions can be significant when dealing with micropores.

The problem of the prediction or interpretation of a distribution coefficient value can lead to either of two situations, according to whether or not the particle-particle interactions must be taken into consideration. At very low concentrations, only the interactions between the pore and single, isolated particles are relevant. This is the Henry's law regime, in which the partition coefficient remains a constant, the Henry's law constant. The range of concentrations within which Henry's law is valid is primarily determined by the character of the intermolecular forces acting in the system. This range will be extremely narrow in the case of charged species, because of the long-ranged electrostatic interactions, and also if particle adsorption occurs onto heterogeneous sites on the solid surface.

In general, the Henry's law constant can be much greater than unity if the pore walls exert an attractive adsorptive action, and also much less than unity if repulsive forces are present. When neither effect is present and the pore walls simply behave as hard walls, the Henry's law constant is not unity but smaller. This is due to the existence of an excluded volume, adjacent to the pore walls, that is not accessible to the center of the particles due to their finite size, Figure 1. This has been studied in great detail by Giddings et al. (1968) for particles of various shapes inside pores of single and of distributed sizes. The important case of flexible polymer-chain solute molecules has been addressed by Casassa (1967, 1976), Casassa and Tagami (1969), Daoud and de Gennes (1977), and Brochard and de Gennes (1979).

When the concentration is increased to the higher values found in many practical situations, Henry's law no longer holds. In other words, the distribution coefficient becomes concentration-dependent. On one hand, the bulk-phase properties are affected by particle-particle interactions. Even when the particles do not attract or repel each other, they interact due to their mutual impenetrability. Interparticle exclusions cause short-range order in the bulk solution. This ordering effect, however, is even more pronounced inside the pores because the pore walls induce an anisotropic structure, i.e. an incipient layering. The breakdown of Henry's law is thus directly related to the appearance of density inhomogeneities inside the pore, primarily of a region of high concentration in the immediate vicinity of the pore walls. The present work is concerned with the influence of particle-particle interactions on the distribution equilibrium. We have already studied the local effects and reported results for the concentration profiles inside pores of various shapes (Glandt, 1980), profiles which are necessary for the estimation of transport coefficients inside pores and membranes (Anderson and Quinn, 1974; Brenner and Gaydos, 1977).

The concentration dependence of the distribution coefficient is a well-established experimental fact (Satterfield et al., 1978). It has been attributed, in many cases, either to adsorption inside the pores or to changes in the intramolecular configuration of the molecules upon entering the pores. These explanations, although plausible for some systems, do not follow from the concentration dependence, since the same effect is also characteristic of rigid, nonadsorbing particles. The important question of distinguishing whether adsorption is or is not present in a given physical system, and of whether the porous material exerts an influence other than just through pore size, must be answered quantitatively. A main test, which the results presented here intend to make possible, is whether the measured concentration levels inside the pores are above what should be expected for nonadsorbing solute molecules.

The virial-type approach to the properties of solutions enclosed by solid walls developed by Bellemans (1962) allows us to introduce successive corrections to Henry's law, corresponding to the simultaneous interaction of two, three, etc., solute molecules. The following sections review the virial treatment of interfacial effects for the case of a pure fluid and of a single-solute solution, respectively. We also present our results for the virial expansion of the partition coefficient for three pore shapes: a parallel-walled slit, a cylindrical pore, and a spherical cavity.

DISTRIBUTION COEFFICIENT FOR A NONADSORBING PURE FLUID

The starting point in the virial treatment of a bulk fluid is to postulate that the logarithm of the grand partition function can be expanded in a power series in the density:

$$\ln \Xi = V \sum_{k=1}^{\infty} B_k c_b^k \tag{1}$$

where B_k is the k-th virial coefficient, and $B_1 = 1$. The virial coefficients can be found, in principle, as integrals involving the intermolecular forces. Their units are chosen here in such a way that c_b represents the molar density or concentration of the fluid. The partition function is related to the thermodynamic properties of the fluid by the fundamental relation of grand ensemble theory, which identifies $RT \ln \Xi$ with the sum of the products of the acting generalized forces and their conjugate generalized displacements. For a pure bulk fluid this is simply

$$RT \ln \Xi = pV \tag{2}$$

We consider now the case where the fluid is contained inside a small pore or cavity. The hard wall of the pore, Σ, encloses a volume V as shown in Figure 1. Inside Σ lies the surface of closest approach, Σ', which encloses the effective volume V' accessible to the center of the molecules. Eq. 1 is formally valid in this case, but the virial coefficients become unwieldy functions of the pore geometry. Bellemans (1962) succeeded in separating the coefficients of Eq. 1 into two parts, one containing "volume" contributions, i.e. the purely intermolecular effects (still characterized by the bulk virial coefficients B_k) and a second part due to interfacial effects. The expansion becomes

$$\ln \Xi = (V + B_{w1}) \sum_{k=1}^{\infty} B_k c_b^k + \sum_{m=2}^{\infty} B_{wm} c_b^m \tag{3}$$

The quantities B_{wm} are the wall-particle virial coefficients, which are calculable in terms of intermolecular and wall-particle forces. For hard-walled pores, the coefficient B_{w1} is simply the negative of the so-called excluded volume, V-V'. Thus, the factor $V + B_{w1}$ can also be written as V'.

In general, the density of the fluid in equilibrium inside the cavity will be nonuniform, although its chemical potential and activity will be the same throughout. The quantity c_b in Eq. 3 represents the limiting molar density far from the walls, i.e., the density of a bulk phase in equilibrium with the fluid inside the pore. For large pores, this density will also be found in some regions of the pore itself. In the presence of a boundary the fundamental relation (Eq. 2), must be written as:

$$RT \ln \Xi = pV - \gamma A \tag{4}$$

where γ is the surface tension. It must be recalled that for other than flat boundaries the choice of the area A, and thus of γ, will not be unique. A comparison of Eqs. 3 and 4 allows us to identify:

$$\frac{pV}{RT} = V' \sum_{k=1}^{\infty} B_k c_b^k \tag{5}$$

and

$$\frac{\gamma A}{RT} = - \sum_{m=2}^{\infty} B_{wm} c_b^k \tag{6}$$

The distinction between bulk and surface contributions to the partition function implied by Eqs. 5 and 6 is not the only possible separation, but it is the most convenient. The equilibrium number of moles inside the pore is found from the basic relation

$$n = \left(\frac{\partial \ln \Xi}{\partial \ln a}\right)_{T,V} \tag{7}$$

and it is a quantity defined without ambiguity. The variable a in Eq. 7 represents the uniform activity of the fluid, which is related to the (also uniform) molar chemical potential of the fluid by:

$$d\mu = RT \, d\ln a \tag{8}$$

Eq. 8 does not suffice to uniquely determine a. Although a complete definition of a is not necessary for the purposes of Eq. 7, it requires that a standard state of unit activity also be adopted. We choose such a state to be the ideal gas bulk phase at unit molar concentration and at the same temperature, so that:

$$\lim_{c_b \to 0} \frac{a}{c_b} = 1 \tag{9}$$

The resulting activity, thus, has the units of a molar concentration. This definition is related to the commonly used fugacity of the fluid by $a = f/RT$. The fugacity scale is an activity scale also, but is based on the so-called reference state: the ideal-gas fluid at unit pressure and at the same temperature. From Eqs. 3 and 7, the following result is derived (Bellemans, 1962):

$$n = V' c_b + \frac{\sum_{m=2}^{\infty} m B_{wm} c_b^m}{\sum_{k=1}^{\infty} k B_k c_b^{k-1}} \tag{10}$$

The leading term in Eq. 10, of first order in the equilibrium bulk concentration, contains the exclusion effect due to the hard pore walls. The higher-order terms are associated with interparticle effects. B_{wm} reflects the influence of the simultaneous interaction of m molecules and the pore walls.

The denominator in Eq. 10 contains the virial coefficients of the unbounded bulk fluid. The first seven coefficients for the hard-sphere gas are shown in Table 1 (Kratky, 1977). The virial equation of state for the unbounded fluid is:

$$\frac{p}{c_b RT} = \sum_{k=1}^{\infty} B_k c_b^{k-1} \tag{11}$$

with, as usual, $B_1 = 1$. Thus, the denominator in Eq. 10 can be readily identified as the dimensionless isothermal bulk modulus of the fluid

$$\frac{1}{RT}\left(\frac{\partial p}{\partial c_b}\right)_T = \sum_{k=1}^{\infty} k B_k c_b^{k-1} \tag{12}$$

whose inverse is the dimensionless isothermal compressibility $\kappa_T^* = RT(\partial c_b/\partial p)_T$; and we rewrite Eq. 10 as:

$$n = V' c_b + \kappa_T^* \sum_{m=2}^{\infty} m B_{wm} c_b^m \tag{13}$$

TABLE 1. VIRIAL COEFFICIENTS FOR A FLUID OF HARD-SPHERICAL PARTICLES OF DIAMETER d: COEFFICIENTS TABULATED IN THE DIMENSIONLESS FORM, $B_k^* = B_k (N_A d^3)^{k-1}$.

k	B_k^*
2	2.0944
3	2.7416
4	2.6362
5	2.1219
6	1.5676
7	1.1563

For computational purposes, it is convenient to replace the series expansion of the compressibility of the bulk fluid with an expression in closed form. The most widely accepted (and a very accurate) equation of state for a fluid of hard particles is the one proposed by Carnahan and Starling (1969),

$$\frac{p}{c_b RT} = \frac{1 + \eta + \eta^2 - \eta^3}{(1 - \eta)^3} \tag{14}$$

where the packing fraction of the bulk phase is defined as $\eta = \pi c_b d^3 N_A/6$, with d being the hard-sphere diameter and N_A Avogadro's number. From Eq. 14, the reduced compressibility is found to be:

$$\kappa_T^* = \frac{(1 - \eta)^4}{1 - 4\eta + 4\eta^2 - 4\eta^3 + \eta^4} \tag{15}$$

It is of interest also to include here the corresponding expression for the activity of the bulk fluid of molar density c_b, as obtained from the same equation of state, since it is also the uniform activity inside the pore. If the activity is defined by Eqs. 8 and 9, by standard thermodynamic manipulations:

$$a = c_b \exp\left[\frac{8\eta - 9\eta^2 + 3\eta^3}{(1 - \eta)^3}\right] \tag{16}$$

A commonly used parameter in the study of phase equilibria is the distribution coefficient K. It is defined here as the ratio between the average molar density $\bar{c} = n/V$ inside the pore and the concentration in the bulk phase, and from Eq. 13 it is

$$K = \frac{\bar{c}}{c_b} = \frac{V'}{V} + \frac{\kappa_T^*}{V} \sum_{m=2}^{\infty} m B_{wm} c_b^{m-1} \tag{17}$$

which can be written in the form

$$K = K_o + K_1 c_b + K_2 c_b^2 + \ldots \tag{18}$$

where $K_o = V'/V$ is the Henry's law constant for the pore phase-bulk phase equilibrium.

When dealing with fluids surrounded by nonmicroporous solid walls, it is customary to express the equilibrium conditions in the form of an adsorption isotherm $\Gamma(c_b)$, where the surface excess is

$$\Gamma = \frac{n - Vc_b}{A} \tag{19}$$

In the case of micropores, however, the adsorption process is one of volume filling rather than of surface covering, and the use of $K(c_b)$ is preferred here to that of $\Gamma(c_b)$.

DISTRIBUTION COEFFICIENT FOR A SOLUTE SPECIES

The virial expansion represented by Eq. 1 is strictly applicable to gases at low and moderate densities. McMillan and Mayer (1945) showed that there is a one-to-one formal corre-

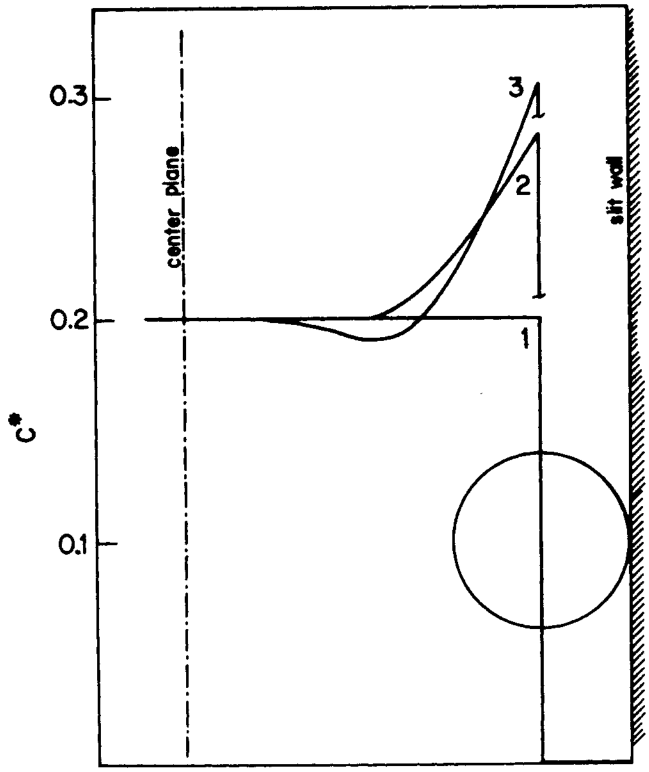

Figure 2. Concentration profile for hard spherical particles in a narrow slit. The ordinate represents the dimensionless molar concentration $c^* = cd^3N_A$.

spondence between an imperfect gas and a dilute solution. The intermolecular potential, which enters into the computation of the gas-phase virial coefficients, must now be replaced by the interaction between two solute molecules, averaged over all the possible configurations of the solvent molecules around them. The solute-solute virial coefficients are the so-called osmotic virial coefficients $B_k(\mu_o, T)$, where μ_o is the chemical potential of the solvent. For a bulk solution in which the molar concentration of the solute is c_b, the McMillan-Mayer analogue of Eq. 1 is:

$$\ln \frac{\Xi}{\Xi_o} = V \sum_{k=1}^{\infty} B_k c_b^k \tag{20}$$

where Ξ_o denotes the grand partition function of the pure solvent at the same chemical potential as in the solution. The left-hand side of Eq. 20 thus represents the change due to the addition of the solute. In grand ensemble theory, this change must be proportional to the osmotic pressure Π:

$$RT \ln \frac{\Xi}{\Xi_o} = \Pi V \tag{21}$$

When the solution is enclosed by a boundary or interface, as happens inside a pore, the addition of the solute will also cause a change in the interfacial tension:

$$RT \ln \frac{\Xi}{\Xi_o} = \Pi V - (\gamma - \gamma_o) A \tag{22}$$

where γ_o is the interfacial tension of the pure solvent at the same chemical potential as in the solution, and where A is the surface area of the interface. Bellemans (1962) separated the bulk and interfacial effects of solute addition on the virial coefficients of Eq. 20:

$$\ln \frac{\Xi}{\Xi_o} = (V + B_{w1}) \sum_{k=1}^{\infty} B_k c_b^k + \sum_{m=2}^{\infty} B_{wm} c_b^m \tag{23}$$

where the B_k are still the bulk osmotic virial coefficients, and where the B_{wm} are the wall-solute virial coefficients. The B_{wm} are also based on solvent-averaged interactions. A comparison of Eqs. 22 and 23 yields the identifications,

$$\Pi = RT \sum_{k=1}^{\infty} B_k c_b^k \tag{24}$$

$$\frac{(\gamma - \gamma_o)A}{RT} = -B_{w1} \sum_{k=1}^{\infty} B_k c_b^k - \sum_{m=2}^{\infty} B_{wm} c_b^m \tag{25}$$

Eq. 24 is the virial osmotic equation of state. Obviously, $B_1 = 1$, since Van't Hoff's equation holds in the very dilute limit. The number of moles of solute inside a pore in equilibrium with a bulk phase of concentration c_b can be obtained by differentiation of Eq. 23 and is (Bellemans, 1962):

$$n = (V + B_{w1}) c_b + \frac{\sum_{m=2}^{\infty} m B_{wm} c_b^m}{\sum_{k=2}^{\infty} k B_k c_b^{k-1}} \tag{26}$$

The distribution coefficient can be defined by:

$$K = \frac{\bar{c}}{c_b} = 1 + \frac{B_{w1}}{V} + \frac{\kappa_1^*}{V} \sum_{m=2}^{\infty} m B_{wm} c_b^m \tag{27}$$

where $\bar{c}$ is the average solute concentration in the pore, and where κ_1^* is now defined as:

$$\kappa_1^* = \frac{1}{RT} \left(\frac{\partial \Pi}{\partial c_b} \right)_T \tag{28}$$

As in the pure-fluid case, Eq. 27 can be viewed as a virial-type expansion of the distribution coefficient:

$$K = K_o + K_1 c_b + K_2 c_b^2 + \ldots \tag{29}$$

where the leading term is the Henry's law constant which, for a pore with hard, nonadsorbing walls, is $K_0 = V'/V$. Eq. 29 can be expressed in dimensionless form by defining a reduced bulk concentration $c_b^* = c_b d^3 N_A$, where N_A is Avogadro's number, and the dimensionless coefficients are $K_n^* = K_n/(d^3N_A)^n$. Thus,

$$K = K_o + K_1^* c_b^* + K_2^* c_b^{*2} + \ldots \tag{30}$$

Eq. 27 represents a virial-type expansion of the average concentration inside the pore. The same type of expansion is also possible for the local concentration $c(\underset{\sim}{r})$ inside the pore, and it has the general form (Bellemans, 1962):

$$c(\underset{\sim}{r}) = e^{-v(\underset{\sim}{r})/kT} c_b [1 + c_b y_1(\underset{\sim}{r}) + c_b^2 y_2(\underset{\sim}{r}) + \ldots] \tag{31}$$

where $v(\underset{\sim}{r})$ is the wall-particle potential, and where k is Boltzmann's constant. From Eqs. 29 and 31, it is obvious that

$$\frac{\kappa_1^*}{V} m B_{wm} \equiv K_m = \frac{1}{V} \int_V e^{-v(\underset{\sim}{r})/kT} y_m(\underset{\sim}{r})\, d\underset{\sim}{r} \tag{32}$$

We have recently calculated and reported (Glandt, 1980) the coefficient functions $y_1(\underset{\sim}{r})$ and $y_2(\underset{\sim}{r})$ for hard-spherical molecules inside pores of three shapes: a flat slit, an infinitely long circular cylinder, and a spherical cavity. We have used those functions in Eq. 32 to obtain K_1 and K_2 directly for the three cases, and the results are presented in the following sections.

FLAT SLIT

Consider a fluid of hard spheres of diameter d placed in the infinite region bounded by two parallel hard walls separated by a distance D. These spheres can be viewed as a pure fluid or as solute molecules embedded in a solvent. The pore region is assumed to be in thermodynamic equilibrium with a bulk phase of hard spheres, of molar concentration c_b. The system is characterized by the dimensionless ratio $d/D = \lambda = \mu^{-1}$.

Figure 2 displays the concentration profile inside a slit for the case $\lambda = 0.2$ and for an equilibrium bulk concentration $c_b^* = N_A d^3 c_b = 0.2$. This concentration value corresponds to a solute volume fraction of approximately 10%. The curves 1, 2, and 3 in Figure 2 are from our previous calculations (Glandt, 1980) which, in turn, are based on the single-wall results of Fischer (1978). These curves show the results of Eq. 31 when truncated after the first-, second-, and third-order terms, respectively. Note that curve 1 accounts only for the effects of the interactions of single particles with the pore walls, and it simply yields the bulk concentration value, except in the vicinity of the walls, where the steric exclusion effect is observed.

The addition of the higher-order terms introduces the particle-particle interaction effects, and shows that indeed there exists an increased concentration in the vicinity of the wall, which cannot be ignored. The third-order term, in particular, produces a "valley" or slightly depleted region, which is evidence of incipient particle layering caused by the wall, even at these relatively low concentrations.

The various terms in the expansion of the partition coefficient K, Eq. 30, reflect the same effects as the terms in Eq. 31. The leading term is the Henry's law constant,

$$K_o = 1 - \lambda \tag{33}$$

and is entirely due to the steric exclusion of single particles. The next two coefficients are more conveniently expressed as Laurent series in $\mu = \lambda^{-1}$

$$K_1 = \frac{\pi}{2\mu} \qquad \mu > 2 \tag{34a}$$

$$= \frac{\pi}{6}\left[\mu^3 - 4\mu^2 + 16 - \frac{13}{\mu}\right] \qquad 1 < \mu < 2 \tag{34b}$$

$$K_2 = \frac{-113}{840}\frac{\pi^2}{\mu} \qquad \mu > 3 \tag{35a}$$

$$= \frac{\pi^2}{8640}\left[\frac{337707}{7\mu} - 41310 - 8901\mu + 19420\mu^2 - 6885\mu^3 + 642\mu^4 + 85\mu^5 - \frac{96}{7}\mu^6\right] \qquad 2 < \mu < 3 \tag{35b}$$

The calculation for K_2 for $1 < \mu < 2$ is a very difficult task. An approximation can be easily constructed, since K_2 and its first derivative must be continuous everywhere, and also K_2 must vanish for $\mu = 1$. The approximation is:

$$K_2 \simeq \frac{1287\,\pi^2}{80640}(\mu^2 - 5\,\mu + 4) \qquad 1 < \mu < 2 \tag{36}$$

The limiting case of $\mu \rightarrow 1$ (or of $\lambda \rightarrow 1$) may also be considered from an entirely different viewpoint. When the slit width is only slightly greater than the diameter of the particles, the centers of the particles are constrained to the immediate vicinity of the midplane of the slit. They become, essentially, a two-dimensional system. When seen in projection, this system is equivalent to a fluid of hard disks (i.e., two-dimensional hard spheres). The particles are thus "adsorbed" in the narrow potential well between the two hard walls.

It is common practice in the study of such adsorbed monolayers to postulate that the external contribution to the thermodynamic properties of the fluid is separable into a contribution from the two degrees of freedom parallel to the monolayer, and another contribution from the very restricted motion in the direction perpendicular to the walls. In this context (Steele, 1974), the activity of the adsorbed phase is:

$$a = (DK_o)^{-1}\, c_2\, \phi_2 \tag{37}$$

The last two factors constitute the parallel contribution: c_2 is the two-dimensional, or superficial, molar concentration and ϕ_2 is a two-dimensional fugacity coefficient. We can calculate ϕ_2 from

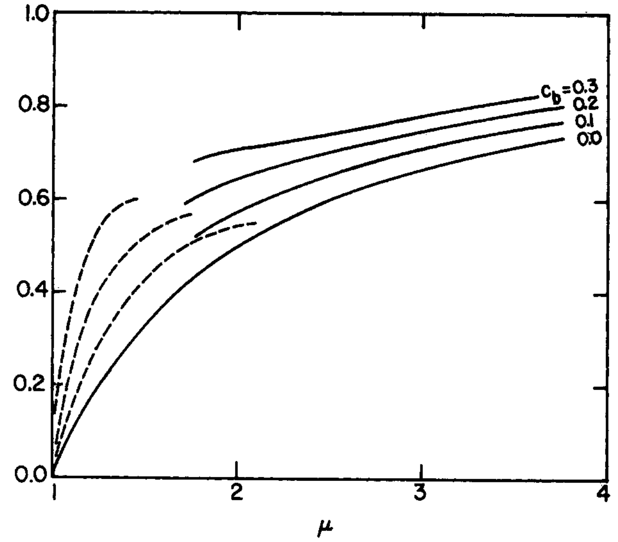

Figure 3. Distribution coefficient between a narrow slit and a bulk phase as a function of $\mu = D/d$. Each slit is in equilibrium with a bulk phase of reduced molar concentration $c_b^* = c_b d^3 N_A$. The solid curves are the result of the exact expansion, i.e., Eqs. 33 to 35. The dashed lines represent an approximation based on a two-dimensional model for the case of slits with $\mu < 2$.

the knowledge of an equation of state for the hard-disk fluid. We adopt here the equation proposed by Henderson (1977):

$$\frac{p_2}{c_2RT} = \frac{(1 - \eta_2)(1 + 0.128\,\eta_2^2) - 0.043\,\eta_2^3}{(1 - \eta_2)^3} \tag{38}$$

where p_2 is the two-dimensional pressure, or spreading pressure, and where η_2 is the two-dimensional packing fraction:

$$\eta_2 = \frac{\pi}{4} N_A\, c_2\, d^2 \tag{39}$$

N_A being Avogadro's number. The two-dimensional molar concentration c_2 is simply related to the average (three-dimensional) molar concentration by:

$$c_2 = D\,\bar{c} \tag{40}$$

Henderson's equation of state, Eq. 38, is in excellent agreement with computer simulations of the hard-disk fluid, and it can be regarded as almost exact at all fluid densities. Standard thermodynamic manipulations on Eq. 38 yield:

$$\phi_2 = (1 - \eta_2)^{-0.743} \exp\left\{\frac{1.257}{1 - \eta_2} - 0.043\left[(1 - \eta_2) + \frac{\eta_2^4}{(1 - \eta_2)^3}\right] + \frac{0.9785 + 0.128\eta_2^2}{(1 - \eta_2)^2} - 2.1925\right\} \tag{41}$$

The quantity $DK_o = D - d$ in Eq. 37 is the "perpendicular" contribution to the activity a, and it vanishes when $\lambda \rightarrow 1$. If we substitute Eqs. 40 and 41 into Eq. 37, an expression for the activity in the pore results, of the form,

$$a = \bar{c}\,\frac{\mu}{\mu - 1}\,\phi_2 \tag{42}$$

At equilibrium, this expression for the activity of the hard-spherical particles inside the pore may be equated to their activity in the bulk phase, as given by Eq. 16. The resulting algebraic equation must be solved numerically for each value of c_b to obtain the corresponding $\bar{c}$ and thus the partition coefficient $K = \bar{c}/c_b$.

Figure 3 shows the partition coefficient as a function of $\mu = D/d$ for several values of c_b^*. The solid lines indicate the exact results. Again, we notice that the concentration dependence, i.e., the effect of particle-particle interaction, is important. For $\mu < 2$, we have also plotted the two-dimensional approximation

TABLE 2. DISTRIBUTION COEFFICIENT FOR HARD-SPHERICAL PARTICLES BETWEEN A CYLINDRICAL PORE AND A BULK PHASE: RESULTS FOR THE COEFFICIENTS IN EQ. 30 FOR DIFFERENT VALUES OF $\lambda = d/D$.

λ	K_1^*	K_2^*
0.1	0.28245	−0.2648
0.2	0.50002	−0.4048
0.3	0.64946	−0.3985
0.4	0.72474	−0.1767
0.5	0.71111	0.3615
0.6	0.56504	0.6940
0.7	0.35163	0.5775
0.8	0.16366	0.3029
0.9	0.04169	0.0809

represented by Eqs. 16, 41, and 42. It can be observed that this approximation appears to continue the exact curves for small values of μ, i.e., for very narrow slits, but that it breaks down, as it should, when μ approaches the value of 2, the value at which the system completely looses its quasi-two-dimensional character. This breakdown occurs sooner for more concentrated systems.

CYLINDRICAL PORE

The coefficients $y_1(\underline{r})$ and $y_2(\underline{r})$ for pores of cylindrical and spherical shapes have been computed numerically and reported earlier (Glandt, 1980). The Percus-Yevick approximation (for example, Barker and Henderson, 1976) was used to avoid some very cumbersome integrations over the relative configurations of clusters of three particles simultaneously interacting with each other and with the pore walls. The Percus-Yevick approximation is known to be very accurate in dealing with short-ranged repulsive potentials, such as that of hard spheres. The error introduced by this approximation is probably a slight underestimate of the particle concentration in the immediate adjacency of the walls.

We consider, then, a system of hard spheres of diameter d placed inside an infinitely long circular cylindrical pore of diameter $D = \mu d = d/\lambda$ and in equilibrium with a bulk phase of hard particles of molar concentration c_b. The partition coefficient $K = \bar{c}/c_b$ relates the average concentration $\bar{c}$ inside the pore (referred to the total pore volume V) to the bulk concentration, and can be expanded as in Eq. 30. The leading term is the Henry's law constant,

$$K_o = (1 - \lambda)^2 \tag{43}$$

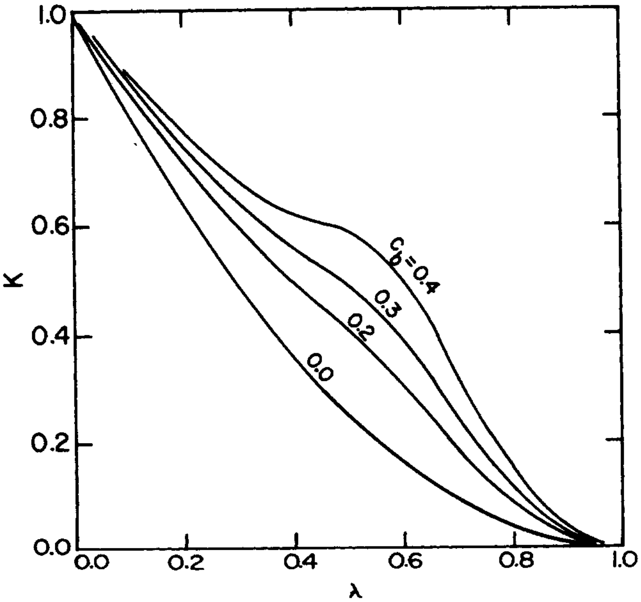

Figure 4. Distribution coefficient between a cylindrical pore and a bulk phase as a function of $\lambda = d/D$. The parameter of the curves is the dimensionless bulk concentration $c_b^* = c_b d^3 N_A$.

The next coefficient in Eq. 30, K_1, was calculated numerically and is shown in Table 2 for different values of λ. These results are essentially exact; the number of figures reported reflects our estimate of the numerical accuracy. The coefficient K_2 was also calculated numerically but with the aid of the Percus-Yevick approximation, Table 2. Figure 4 shows the partition coefficient K as a function of λ for various values of c_b^*. As in the flat-slit case, the effect of concentration is appreciable, and it is most important at intermediate values of λ.

When λ is very small, i.e., when the pore diameter is relatively very large, the curvature of the wall may be neglected. The concentration profile near the wall becomes essentially the one found near a flat wall, which is known (Fischer, 1978). The introduction of this profile into Eq. 32 yields:

$$K_1^* \simeq \pi \left(\lambda - \frac{23}{15}\lambda^2\right) \quad \text{as } \lambda \to 0 \tag{44}$$

Likewise, the Percus-Yevick estimate of K_2 shows the following behavior at low λ:

$$K_2^* \simeq \pi^2 \left(\frac{-\lambda}{3} + \lambda^2\right) \quad \text{as } \lambda \to 0 \tag{45}$$

The other limiting situation, that of $\lambda \to 1$ or of very narrow pores, can also be studied in great detail and at all densities, as in the case of the flat slit. Indeed, when the diameter of the pore is only slightly greater than that of the particles, the centers of the particles must lie very close to the pore axis, behaving effectively as a fluid of "hard rods." The hard-rod fluid, the one-dimensional equivalent of the hard-sphere model, is a very rare example of a model substance whose properties can be exactly solved for. As before, the thermodynamic properties of the fluid inside the pore can be separated into two parts: an axial and a radial component. In particular, the activity can be written as:

$$a = K_H^{-1}\, c_1\, \phi_1 \tag{46}$$

where c_1 is the linear molar concentration of particles along the pore axis, related to the average (three-dimensional) concentration within the pore by:

$$c_1 = \frac{\pi}{4} D^2 \bar{c} \tag{47}$$

The quantity K_H in Eq. 46 is the radial contribution, i.e., the Henry's law constant for this "line adsorption" process:

$$K_H = \frac{\pi}{4} D^2 (1 - \lambda)^2 \tag{48}$$

The factor $\phi_1(c_1)$ in Eq. 46 represents the one-dimensional fugacity coefficient of the hard-rod fluid, and it can be readily calculated from the equation of state of this fluid (Tonks, 1936):

$$\frac{p_1}{c_1 RT} = \frac{1}{1 - \eta_1} \tag{49}$$

with p_1 being the one-dimensional pressure, i.e., simply a force, and η_1 the one-dimensional packing fraction:

$$\eta_1 = c_1\, N_A\, d \tag{50}$$

This coefficient ϕ_1 is found to be:

$$\phi_1 = \frac{1}{1 - \eta_1} \exp\left(\frac{\eta_1}{1 - \eta_1}\right) \tag{51}$$

Substitution of Eqs. 47, 48, and 51 into Eq. 46 yields the activity of the particles inside the pore as a function of the average density $\bar{c}$:

$$a = \left(\frac{4\lambda^2}{(1-\lambda)^2}\right)\bar{c}\,\frac{\exp\left[\dfrac{\pi\,\bar{c}\,d^3}{4\lambda^2 - \pi\bar{c}d^3}\right]}{(4\lambda^2 - \pi\bar{c}d^3)} \tag{52}$$

Recall that the activity has the dimensions of a regular molar concentration. When equated to the activity of the bulk fluid in equilibrium with the pore, Eq. 16, a relationship between $\bar{c}$ and c_b results, which determines $K(c_b)$.

The one-dimensional model for particles in a cylindrical pore when $\lambda \rightarrow 1$ corresponds to the so-called "single file" or "in-line" diffusion model for transport across pores and membranes (Heckmann, 1972). It has been advocated that this picture of solute molecules that cannot overtake other solute particles within a pore is commonly realized in biological membranes and might be responsible for their great selectivity. The introduction here of the one-dimensional approximation simply provides us with a separate method for the calculation of $K(c_b)$ in the $\lambda \rightarrow 1$ limit, a method that, unlike the virial approach, is valid at all concentrations. In addition, other useful information can also be obtained from the hard-rod model. Most interesting is the relative distribution of particles in equilibrium along the pore axis, i.e., the pair correlation function. This distribution was first derived by Salzburg et al. (1953), and a short and elegant derivation was also offered by Pickard and Tory (1979) very recently. Consider a particle at any position on the pore axis. The local linear concentration of other particles at a distance x from the first one, measured along the axis, is given by the sum over the probabilities that these other particles be the first-, second-, . . . k-th nearest neighbors of the first particle:

$$c_{1,\text{local}}(x) = \sum_{k=1}^{[x/d]} f_k\left(\frac{x}{d}\right) \tag{53}$$

where $[x]$ denotes the largest integer less than or equal to x, and where the distribution of k-th nearest neighbors is:

$$f_k\left(\frac{x}{d}\right) = \left(\frac{c_1 d}{1 - c_1 d}\right)^k \left[\frac{\left(\frac{x}{d} - k\right)^{k-1}}{(k-1)!}\right] \exp\left[\frac{c_1(kd - x)}{1 - c_1 d}\right] \quad \text{for } k < \frac{x}{d} \tag{54}$$

$$= 0 \qquad \text{for } k > \frac{x}{d}$$

Also, the gap length ℓ between neighboring particles along the pore axis is distributed with a Poisson-type probability density

$$P(\ell) = c_1\, e^{-c_1 \ell} \tag{55}$$

Figure 5 compares the partition coefficient obtained from Eq. 30 and the data in Table 2 (solid line) with the one-dimensional model (dashed line) as functions of λ and for a reduced bulk concentration $c_b^* = 0.2$. Also included, as a reference, is the low-concentration limit $K_o = (1 - \lambda)^2$. The hard-rod model is seen to provide an excellent approximation for $\lambda > 0.5$, i.e., for those cases when one particle cannot overtake another one inside the pore. There seems to be a small systematic difference between the solid and dashed lines in Figure 5, even when λ is very close to unity. This effect might be due to the Percus-Yevick approximation, which would tend to lower the solid line and to the neglect of higher-order terms in Eq. 30.

SPHERICAL CAVITY

Consider now a fluid of hard spheres of diameter d contained inside a spherical cavity of diameter D and in equilibrium with a bulk phase of molar concentration c_b. We need not consider whether the pore-bulk equilibrium is established via openings in the cavity wall or through other mechanism. The partition coefficient can again be expanded as in Eq. 30, where the Henry's law constant is:

$$K_o = (1 - \lambda)^3 \tag{56}$$

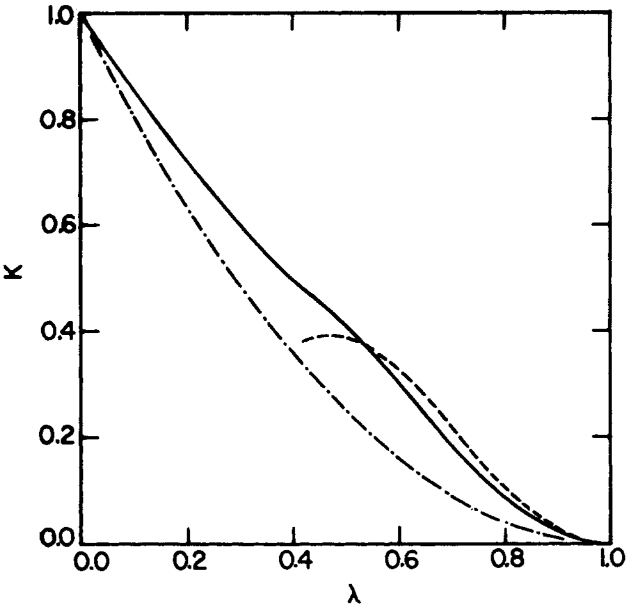

Figure 5. Distribution coefficient between a cylindrical pore and a bulk phase for $c_b^* = 0.2$. The solid line is the result of the virial calculation using the coefficients of Table 2. The dashed line is the result of the one-dimensional approximation, using the hard-rod model described in the text. The lower line is the low-concentration limit, K_o.

TABLE 3. DISTRIBUTION COEFFICIENT FOR HARD-SPHERICAL PARTICLES BETWEEN A SPHERICAL CAVITY AND A BULK PHASE: RESULTS FOR THE COEFFICIENTS IN EQ. 30. THE COEFFICIENT K_2^* WAS ESTIMATED WITH THE AID OF THE PERCUS-YEVICK APPROXIMATION.

	K_1^*	K_2^*
0.1	0.38066	−0.32816
0.2	0.59481	−0.35531
0.3	0.66445	−0.12584
0.4	0.61156	0.30659
0.5	0.45815	0.61652
0.6	0.25815	0.45529
0.7	0.11198	0.21356
0.8	0.03344	0.06527
0.9	0.00419	0.00821

The next coefficient, K_1, was calculated numerically as in Eq. 32 and the results are shown in Table 3 for different values of $\lambda = d/D$. For $\lambda > 0.5$, this coefficient is given by:

$$K_1 = \frac{\pi}{6}(-9\lambda^3 + 30\lambda^2 - 39\lambda + 28 - 15\lambda^{-1} + 6\lambda^{-2} - \lambda^{-3}) \tag{57}$$

The coefficient K_2 was computed with the aid of the Percus-Yevick approximation, and is also shown in reduced form in Table 3. Figure 6 shows the partition coefficient K between the spherical cavity and a bulk phase as a function of λ for various values of the reduced bulk concentration. The curves are qualitatively very similar to the corresponding plot for a cylindrical pore, Figure 4, and the effect of concentration is seen to be also significant here.

For very small values of λ, the curvature of the wall may be neglected and the concentration profiles near a flat wall used in Eq. 32 to obtain

$$K_1^* \simeq \frac{\pi}{30}(45\lambda - 138\lambda^2 + 113\lambda^3) \quad \text{as } \lambda \rightarrow 0 \tag{58}$$

and

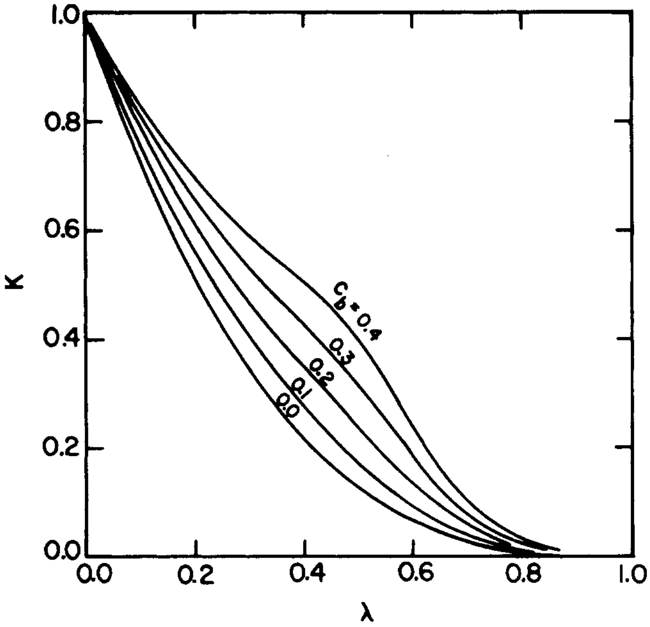

Figure 6. Distribution coefficient between a spherical cavity and a bulk phase as a function of $\lambda = d/D$. The parameter of the curves is the dimensionless bulk concentration $c_b^* = c_b d^3 N_A$.

$$K_2^* \simeq \frac{\pi^2}{10}(-5\lambda + 30\lambda^2 - 43\lambda^3) \quad \text{as } \lambda \to 0 \tag{59}$$

Eq. 59 still assumes the Percus-Yevick approximation.

DISCUSSION

The results presented above would certainly be altered if the interactions between the pore walls and the individual particles were different from the hard, nonattractive potential considered here. For nonuniform potentials, it would no longer be possible to uniquely define V or V'. The Henry's law constant must then be calculated from the wall-particle potential $v(\underline{r})$ inside the pore as:

$$K_o = \frac{1}{V}\int_V \exp\,[-v(\underline{r})/kT]\,dV \tag{60}$$

and would be a function of the temperature. The integration in Eq. 60 should include all portions of the pore in which the integrand is not vanishingly small. The volume V can then be arbitrarily chosen, as long as this condition is met. Steele and Halsey (1954) performed this integration for an adsorbing potential consisting of a hard-core repulsion plus an attractive part proportional to the inverse cube of the wall-particle distance. Recently, an equivalent calculation was performed by Soto et al. (1980) for adsorption in molecular sieve cavities. They showed how, when only dispersion and repulsion forces are considered, the computations can be approximated by the integrals used in the Lennard-Jones and Devonshire hole theory of liquids.

We are particularly interested here in the case where the particles experience a uniform potential v, either attractive or repulsive, inside the pore, since our results for K_1 and K_2 are still applicable there. The Henry's law constant, as given by Eq. 60, then becomes:

$$K_o = \frac{V'}{V}e^{-v/kT} \tag{61}$$

Eq. 18 is also valid under these conditions, but with the bulk concentration c_b everywhere replaced by the Henry's law value $c_b \exp(-v/kT)$. Although our results are for the simple case of uniformly sized particles and uniformly sized pores, they may also be immediately extended to a distribution of pore sizes (Giddings et al., 1968).

We recall, from Eq. 29, that the value of K is the result of two effects. The steric exclusion, represented by K_o, which is independent of bulk concentration, is always less than unity. The higher-order terms measure the particle-particle interactions, which are different inside the pore and in the bulk due to the layering influence of the pore walls. This latter contribution to K is always positive for hard particles and is best measured by the average excess concentration of particles inside the pore:

$$\bar{c}_{\text{exc}} = \frac{n - c_b V'}{V} \tag{62}$$

From Eqs. 17 and 62, it follows that:

$$\frac{\bar{c}_{\text{exc}}}{c_b} = K - K_o \tag{63}$$

For a given bulk concentration and particle size, $\bar{c}_{\text{exc}}$ is a function of the pore size. Notice that $\bar{c}_{\text{exc}}$ must vanish for the two extreme cases: when the pores are very large ($\lambda \to 0$) and thus the influence of the pore walls is negligible, and also for very small pores ($\lambda \to 1$), in which case, particle-particle interaction effects are severely limited. Therefore, at each bulk concentration, there must exist an intermediate pore size for which $\bar{c}_{\text{exc}}$ is a maximum. The corresponding size ratio, $\lambda_{\max}$, can be determined from Eqs. 29 and 61 and the data for K_1 and K_2. We have done so for the most important case of the cylindrical pore, and found that $\lambda_{\max}$ is well correlated by:

$$\lambda_{\max} = 0.394 + (0.0016 + 0.0521\, c_b^*)^{\frac{1}{2}} \tag{64}$$

ACKNOWLEDGMENT

The author is grateful to the National Science Foundation for financial support of this work under grant ENG78-05410. Useful conversations with J. L. Anderson and J. A. Quinn are also acknowledged.

NOTATION

a = thermodynamic activity
A = surface area
B_k = virial coefficients
B_{wk} = wall-particle virial coefficients
$c(\underline{r})$ = local concentration inside a pore
$\bar{c}$ = average molar concentration inside a pore
c_b = bulk concentration
c_1 = linear molar concentration along a pore axis
c_2 = surface molar concentration in the midplane of a slit
d = hard-sphere diameter
D = diameter or width of a pore
f = fugacity
k = Boltzmann's constant = R/N_A
K = pore-bulk distribution (or partition) coefficient
K_n = coefficients in the virial expansion of K
ℓ = gap length between two particles on the pore axis
n = number of moles contained inside a pore
N_A = Avogadro's number
p = pressure
p_1 = one-dimensional pressure = force
p_2 = two-dimensional pressure = spreading pressure
$\underline{r}$ = position vector inside a pore
R = ideal-gas constant
T = absolute temperature
$v(r)$ = pore-particle interaction potential
V = pore volume
V' = volume accessible to the center of the molecules
x = center-to-center interparticle distance along the pore axis
y_n = coefficients in the concentration expansion of the density profile, Eq. 31

Greek Letters

γ = surface tension
Γ = surface excess, defined by Eq. 19

η = packing fraction in the bulk phase = $\pi c_b d^3 N_A/6$
η_1 = linear packing fraction = $c_1 N_A d$
η_2 = two-dimensional packing fraction = $\pi c_2 d^2 N_A/4$
κ_T = isothermal compressibility
κ_T^* = dimensionless isothermal compressibility = $RT(\partial c_b/\partial p)_T$; group defined by Eq. 28
λ = size ratio = d/D
μ = size ratio = D/d; chemical potential
Ξ = grand-canonical partition function
Π = osmotic pressure
ϕ_1, ϕ_2 = fugacity coefficients for a one- and two-dimensional fluid, respectively

Subscripts

b = bulk phase
o = pure solvent

LITERATURE CITED

Anderson, J. L., and J. A. Quinn, "Restricted Transport in Small Pores," *Biophys. J.*, **14**, 130 (1974).

Barker, J. A., and D. Henderson, "What is Liquid? Understanding the States of Matter," *Rev. Mod. Phys.*, **48**, 587 (1976).

Bellemans A., "Statistical Mechanics of Surface Phenomena," part I, *Physica*, **28**, 493 (1962); part II, *ibid.*, **28**, 617 (1962).

Brenner, H., and L. J. Gaydos, "The Constrained Brownian Movement of Spherical Particles in Cylindrical Pores of Comparable Radius," *J. Colloid Int. Sci.*, **58**, 312 (1977).

Brochard, F., and P. G. de Gennes, "Conformations de Polymeres Fondus dans des Pores Tres Petits," *J. Physique*, **40**, L-399 (1979).

Carnahan, N. F., and K. E. Starling, "Equation of State for Nonattracting Rigid Spheres," *J. Chem. Phys.*, **51**, 635 (1969).

Casassa, E. F., "Equilibrium Distribution of Flexible Polymer Chains between a Macroscopic Solution Phase and Small Voids," *J. Polymer Sci.*, **B5**, 773 (1967).

Casassa, E. F., "Comments on Exclusion of Polymer Chains from Small Pores and Its Relation to Gel Permeation Chromatography," *Macromolecules*, **9**, 182 (1976).

Casassa, E. F., and Y. Tagami, "An Equilibrium Theory for Exclusion Chromatography of Branched and Linear Polymer Chains," *Macromolecules*, **2**, 14 (1969).

Daoud, M., and P. G. de Gennes, "Statistics of Macromolecular Solutions Trapped in Small Pores," *J. Physique*, **38**, 85 (1977).

Fischer, J., "Fourth-Order Interaction of Hard Spheres with a Hard Wall," *Mol. Phys.*, **35**, 897 (1978).

Giddings, J. C., E. Kucera, C. P. Russell, and M. N. Myers, "Statistical Theory for the Equilibrium Distribution of Rigid Molecules in Inert Porous Networks: Exclusion Chromatography," *J. Phys. Chem.*, **72**, 4397 (1968).

Glandt, E. D., "Density Distribution of Hard-Spherical Molecules inside Small Pores of Various Shapes," *J. Colloid Int. Sci.*, **77**, 512 (1980).

Heckmann, K., "Single File Diffusion," *Biomembranes*, K. Kreuzer and J. F. G. Slegers, eds., **3**, Plenum, N.Y., 127 (1972).

Henderson, D., "Monte Carlo and Perturbation Theory Studies of the Equation of State of the Two-Dimensional Lennard-Jones Fluid," *Mol. Phys.*, **34**, 301 (1977).

Kratky, K. W., "Fifth to Tenth Virial Coefficients of a Hard-Sphere Fluid," *Physica*, **87A**, 584 (1977).

McMillan, W. G., and J. E. Mayer, "The Statistical Thermodynamics of Multicomponent Systems," *J. Chem. Phys.*, **13**, 276 (1945).

Pickard, D. K., and E. M. Tory, "The Radial Distribution Function of Hard Rods," *J. Chem. Phys.*, **70**, 5923 (1979).

Salzburg, Z. W., R. W. Zwanzig, and J. G. Kirkwood, "Molecular Distribution Functions in a One-Dimensional Fluid," *J. Chem. Phys.*, **21**, 1098 (1953).

Satterfield, C. N., C. K. Colton, B. de Turckheim, and T. M. Copeland, "Effect of Concentration on Partitioning of Polystyrene within Finely Porous Glass," *AIChE J.*, **24**, 937 (1978).

Steele, W. A., "The Interaction of Gases with Solid Surfaces," Pergamon, Oxford (1974).

Tonks, L., "The Complete Equation of State of One-, Two-, and Three-Dimensional Gases of Hard Elastic Spheres," *Phys. Rev.*, **50**, 955 (1936).

Manuscript received February 12, 1980; revision received April 22, and accepted May 7, 1980.

Gas-Phase Combustion in Fluidized Beds

Kerosine or propane was injected near the base of a small, air-fluidized bed of sand at 940°C. The fraction of fuel burnt within the bed was determined from a heat balance, for various particle sizes, fluidizing velocities, and bed depths.

Assuming the initial formation of a train of fuel vapor bubbles, theoretical analysis indicated two stages of combustion: (1) rapid consumption of the oxygen initially between fuel vapor bubbles; (2) slow consumption of oxygen initially outside the fuel vapor region by radial diffusion of oxygen and fuel vapor, analogous to a diffusion flame.

Comparison of experiment with theory gave effective radial diffusion coefficients of the same order of magnitude as the molecular diffusion coefficient. It was inferred that combustion occurs largely by a diffusion flame within the bed, with diffusion through the particulate phase being the rate-controlling step. This explains why fuel distribution is so important in attaining efficient combustion.

J. F. STUBINGTON

Dept. of Fuel Technology
University of N.S.W.
Sydney, Australia

J. F. DAVIDSON

Dept. of Chemical Engineering
University of Cambridge
Pembroke Street
Cambridge, England

SCOPE

The objective of this work was to elucidate the mechanism of combustion of oil or gas injected at a single point into an air-fluidized bed of inert particles such as sand. Intuition suggests that the high degree of mixing in a violently fluidized bed would facilitate combustion, so that complete combustion would occur within a short distance from the point of injection, provided the fluidizing air supplied was sufficient to burn the fuel.

On the other hand, when oil or gas is injected into an air-fluidized bed, overbed burning may occur unless the number of fuel injection points is adequate, perhaps 1/m² of superficial area for a large industrial fluidized combustor. This work

---

0001-1541-81-4213-0059-$2.00. ©The American Institute of Chemical Engineers, 1981.